

Phonon Drag and Phonon Interactions in  $n$ -InSb†

S. M. PURI

*Microwave Laboratory, Stanford University, Stanford, California*

(Received 9 March 1965)

The experimental results of phonon-drag thermoelectric power of  $n$ -InSb are analyzed to obtain information about electron-phonon and phonon-phonon interactions. We find that for temperatures greater than 6°K, the piezoelectric mode of electron scattering is negligible as compared to the deformation potential type of scattering. A value of 8.25 eV is found for the deformation-potential constant. The relaxation time of long-wavelength acoustical phonons is given by  $\tau_q(T) = 4.4 \times 10^8 / qT^3$  for temperatures  $\tau \leq 40^\circ\text{K}$ . The data also indicate that inelasticity of electron-phonon collisions as well as collision broadening of the electron energy levels are the dominant "cutoff" mechanisms involved in the quantum theory of magnetoresistance; the first dominates in relatively low fields, while the latter takes over for fields greater than 60 kG.

## I. INTRODUCTION

IN a previous paper,<sup>1</sup> we presented the results of our measurements on the thermoelectric power  $Q$  of  $n$ -type InSb in high magnetic fields up to 100 kG covering a temperature range from 7 to 80°K. We determined the phonon-drag component  $Q_p$ , which is the contribution to the thermoelectric power because of a nonequilibrium phonon distribution that exists in the presence of a temperature gradient. This was done, as usual,<sup>2</sup> by subtracting from the measured values of  $Q$  the calculated value of the electronic component  $Q_e$ . It was concluded in that paper, in agreement with previous works,<sup>3,4</sup> that as long as the magnetic field is in the classical region, i.e.,  $\hbar\omega \ll k_0T$ , the phonon-drag component  $Q_p$  is very small, the maximum value of about 50  $\mu\text{V}/\text{deg}$  being obtained near 20°K. Here,  $\omega$  is the cyclotron frequency of electrons and  $k_0T$  is of the order of energy of a typical conduction electron in a distribution approximated by classical statistics and having temperature  $T$ . The reason for this, it was pointed out, is that the scattering on ionized impurities dominates the momentum-dissipation mechanisms for electrons in InSb below liquid-nitrogen temperatures; a small effective mass of the electron and a relatively weaker interaction with acoustic phonons bring this about. In higher magnetic fields, in the quantum region ( $\hbar\omega \gtrsim k_0T$ ), however, the phonon-drag thermoelectric power  $Q_p$  increases very rapidly with the magnetic field, much more rapidly than the electronic component  $Q_e$ , and makes the dominant contribution to the total thermoelectric power  $Q$  at low temperatures. The extreme sensitivity of the measured value of  $Q$  at about 20°K to the size of the cross section of the specimen confirms this view because only the phonon-drag component, and not the electronic component, is expected

to depend upon the size of the specimen at these temperatures. In the quantum region, the electron scattering on acoustic phonons obviously starts making an important contribution to the momentum-dissipation mechanisms for electrons. A phonon-drag component of  $\sim 10\,000 \mu\text{V}/\text{deg}$  is obtained at 10°K and in a field of 100 kG. This estimate is based on the calculation of the electronic component  $Q_e$ , as presented in Ref. 1, which we may point out differs very much from the previously published calculations.<sup>5</sup> If  $Q_e$  is calculated based on the theory of Ref. 5, then  $Q_p$  is vastly reduced although it still makes an important contribution to  $Q$ . The realization of a large  $Q_p$  makes available<sup>6,7</sup> another method to study electron-phonon and phonon-phonon scattering. The phonons referred to here are the long-wavelength acoustic phonons. In this communication, we analyze the measurements of Ref. 1 to this effect.

The relaxation mechanisms of long-wavelength acoustic phonons in the longitudinal branch are not very well understood. If dispersion of frequency versus wavevector spectrum of the lattice vibrations is taken into account, the scattering events for a long-wavelength phonon in which both the energy- and momentum-conservation laws are satisfied are very few in an elastically isotropic solid. The resultant mean free path is so long that the calculated thermal conductivity due to these modes becomes infinite. Herring<sup>8</sup> was the first to point out that the consideration of elastic anisotropy removes the divergence in thermal conductivity in crystals of certain symmetry groups. He predicted the frequency and the temperature dependence for the mean free path of these phonons. Up till now the most detailed information which can be compared with the theory has come from the phonon-drag thermomagnetic experiments<sup>7,9</sup> and the size dependence of thermal con-

† This work was supported by the U. S. Army Research Office, the U. S. Air Force Office of Scientific Research, and the U. S. Office of Naval Research under the Joint Services Electronics program.

<sup>1</sup> S. M. Puri and T. H. Geballe, Phys. Rev. **136**, A1767 (1964).

<sup>2</sup> (a) H. P. R. Frederikse, Phys. Rev. **91**, 491 (1953); **92**, 248 (1953); (b) T. H. Geballe, *ibid.* **92**, 857 (1953).

<sup>3</sup> H. P. R. Frederikse and E. Mielczarek, Phys. Rev. **99**, 1889 (1955).

<sup>4</sup> T. H. Geballe, Bull. Am. Phys. Soc. **2**, 56 (1957).

<sup>5</sup> A. I. Anselm and B. M. Askerov, Fiz. Tverd. Tela **3**, 3668 (1961) [English transl.: Soviet Phys.—Solid State **3**, 2665 (1962)].

<sup>6</sup> C. Herring, *Halbleiter und Phosphore*, edited by M. Schol and H. Welker (Fredrick Vieweg und Sohn, Braunschweig, 1958), p. 184.

<sup>7</sup> C. Herring, T. H. Geballe, and J. E. Kunzler, Bell System Tech. J. **38**, 657 (1959).

<sup>8</sup> C. Herring, Phys. Rev. **95**, 954 (1954).

<sup>9</sup> C. Herring, T. H. Geballe, and J. E. Kunzler, Phys. Rev. **111**, 36 (1958).

ductivity<sup>10</sup> in *n*-type Ge. However, in the *n*-type Ge, because of the anisotropic energy surfaces both the transverse as well as the longitudinal branches of the phonon spectrum contribute to phonon drag and the information about phonon relaxation time obtained from the experiments relates to a certain average behavior of both these branches. This leaves some element of uncertainty in a detailed comparison with theory because the mean free paths for the two branches are expected to be quite different in magnitude as well as in their dependence on frequency and temperature. Some information has also been obtained from the attenuation of laboratory-generated microwave phonons.<sup>11-15</sup> These measurements, despite the technical problems, have already thrown much light on phonon-phonon scattering. However, the laboratory-generated phonons have much lower frequencies,  $\sim 10^{10}$  cycles/sec. The analysis of high-magnetic-field phonon drag  $Q_p$  yields information about phonons of frequency up to  $10^{12}$  cycles/sec. Since in InSb the electron-energy surfaces are isotropic, it may be expected that only the longitudinal phonons contribute to phonon drag so that there is no mixing of transverse phonons as in the case of *n*-type Ge.

A second motivation for these experiments is to learn about the mechanisms of electron scattering on acoustic phonons in InSb. Usually this information can be obtained from the analysis of electron mobility data. But in the case of InSb, this is difficult. As Ehrenreich<sup>16</sup> has shown, above 200°K electrons are scattered mostly by optical phonons via the polar interaction. Perhaps this type of scattering is important as far down as liquid-nitrogen temperatures.<sup>17,18</sup> As the temperature is reduced further, even in the purest available samples, the scattering on ionized impurities takes over directly from scattering on optical phonons. The existing information about the electron scattering on acoustic phonons is neither very extensive nor very precise. The InSb crystals grow in the cubic zincblende structure which lacks a center of symmetry and, therefore, may be piezoelectric. The strain produced by acoustic phonons in the crystal gives rise to a piezoelectric polarization charge from which the electrons are scattered. Thus, the piezoelectric mode of scattering will be in

addition to the usual deformation-potential-type scattering. The relative amount of electron coupling to either of these mechanisms is not known. Several workers<sup>19,20</sup> have interpreted their experiments to mean that the piezoelectric coupling is much stronger than the deformation-potential-type coupling, while others have taken just the opposite view.<sup>21</sup> There is no direct experimental measurement of either the deformation-potential constant  $\eta_D$  or the piezoelectric-elastic constant  $e_{14}$ . Ehrenreich<sup>16</sup> has estimated the value of  $\eta_D$  from the measured value<sup>22</sup> of the variation of the energy gap with pressure. He assumed that this variation is entirely due to changes in the energy of the conduction-band minima, the valence-band maxima being stationary with respect to strains produced by pressure. He found a value of 7.2 eV for  $\eta_D$ . Recently, Haga and Kimura<sup>23</sup> have analyzed the experiments on free-carrier infrared absorption<sup>24</sup> and find a value of 30 eV for  $\eta_D$ . The phonon-drag experiments can give a more direct measurement of  $\eta_D$ . Indeed we find a value of  $\eta_D$  closer to Ehrenreich's<sup>16</sup> estimate and also that the piezoelectric type of coupling is negligible for  $T \gtrsim 6^\circ\text{K}$ .

The analysis presented in this paper is based on Herring's theory of phonon drag.<sup>6,25</sup> In Sec. II we calculate the phonon drag  $Q_p$  in the quantum region. The procedure is to calculate the energy flux due to the non-equilibrium distribution of phonons that exists in the presence of an electric field under isothermal conditions. The steady-state phonon distribution is obtained using a transport equation for phonons in which the electron-phonon collisions make up the driving term and the phonon-phonon collisions or phonon collisions on the boundaries of the specimen are the relaxation mechanisms. The driving term is calculated after Titeica,<sup>26</sup> using the quantized energy levels and wave functions of an electron in the presence of crossed electric and magnetic fields. It is assumed that all electrons are in the lowest Landau level and the scattering is calculated in the first Born approximation. It turns out, in this approximation, that the presence of electron scattering on ionized impurities does not affect the electron-phonon scattering rate and hence  $Q_p$ .

In Sec. IIA we neglect all band-structure effects and discuss the case of an electron gas interacting with phonon and impurities but otherwise free. The inter-band interactions modify the electron-phonon scattering rate. The band effects make a sizeable correction in the case of *n*-InSb whose conduction band is known to be very nonparabolic.<sup>27</sup> These corrections are considered

<sup>10</sup> T. H. Geballe and G. W. Hull, *Conference de Physique des Basses Températures, Paris, 1955* (Institut International du Froid, Paris, 1955), p. 460.

<sup>11</sup> R. Nava, R. Azrt, I. Ciccarello, and K. Dransfeld, *Phys. Rev.* **134**, A581 (1964).

<sup>12</sup> I. S. Ciccarello and K. Dransfeld, *Phys. Rev.* **134**, A1517 (1964).

<sup>13</sup> H. E. Bommel and K. Dransfeld, *Phys. Rev.* **117**, 1245 (1960).

<sup>14</sup> E. H. Jacobsen, *Phys. Rev. Letters* **2**, 249 (1959); also article in *Quantum Electronics* (Columbia University Press, New York, 1960), p. 468.

<sup>15</sup> S. Simons, *Proc. Phys. Soc. (London)* **83**, 749 (1964).

<sup>16</sup> H. Ehrenreich, *J. Phys. Chem. Solids* **2**, 131 (1957); **9**, 129 (1959); R. F. Potter, *Phys. Rev.* **108**, 652 (1957).

<sup>17</sup> S. M. Puri and T. H. Geballe, *Bull. Am. Phys. Soc.* **8**, 309 (1963).

<sup>18</sup> Yu. A. Firsov, V. L. Gurevich, R. V. Farfaniev, and S. S. Shalyt, *Phys. Rev. Letters* **12**, 660 (1964).

<sup>19</sup> R. J. Sladek, *Phys. Rev.* **120**, 1589 (1960).

<sup>20</sup> G. D. Peskett and B. V. Rollin, *Proc. Phys. Soc. (London)* **82**, 467 (1963).

<sup>21</sup> J. Bok and C. Guthmann, *Phys. Stat. Solidi* **6**, 853 (1964).

<sup>22</sup> R. W. Keyes, *Phys. Rev.* **99**, 490 (1955).

<sup>23</sup> Eijiro Haga and Hatsui Kimura, *J. Phys. Soc. Japan* **18**, 777 (1963).

<sup>24</sup> W. G. Spitzer and H. Y. Fan, *Phys. Rev.* **106**, 882 (1957).

<sup>25</sup> C. Herring, *Phys. Rev.* **96**, 1163 (1954).

<sup>26</sup> S. Titeica, *Ann. Physik* **22**, 129 (1935).

<sup>27</sup> E. O. Kane, *J. Phys. Chem. Solids* **1**, 249 (1956).

in Sec. IIB using Yafet's<sup>28</sup> results for the energy levels of band electrons in the presence of a magnetic field. The electron-phonon scattering rate is reduced because of the modifications of the wave functions by an admixture having the symmetry of the valence-band wave functions. Simple algebraic expressions are used for the relaxation time of phonons describing the phonon-phonon collisions. The Peltier coefficient  $\pi$  is calculated from the electric current and the energy flux carried by phonons; the thermoelectric power is obtained using the Kelvin relation.

The final formulas are listed in Sec. IIC, where we neglect the influence of electron-phonon collisions on the phonon-relaxation time, i.e., we consider the case of an ideal "dilute" semiconductor with no saturation effect.<sup>6</sup> The first-order correction due to a finite electron density, which has been called the saturation effect, is discussed in Sec. IID.

The contribution of the purely electron-diffusion term to the thermoelectric power is briefly reviewed in Sec. III. For the purpose of the analysis presented in this paper, we have essentially used the calculation of  $Q_e$  presented in Ref. 1, but have modified the formulas to take into account the spin splitting of the Landau levels as well as the effects due to the nonparabolic band. We believe that an analysis based on the above theory, though elementary, is quite adequate to obtain useful information from the experiments. A few details of the experiment are given in Sec. IV to supplement the information given in Ref. 1. In Sec. V we compare the results of experiment and the theory. The bearing of the results on the relative magnitudes of the piezoelectric versus deformation-potential scattering is discussed in Sec. VA. The frequency and the temperature dependence of the phonon relaxation time is discussed in Sec. VI. The conclusions of the analysis are summarized in Sec. VII.

## II. THEORY OF PHONON-DRAG THERMOELECTRIC POWER

In a preferentially heated solid, phonons drift along the gradient of temperature. This phonon current, by reason of its interaction with electrons, exerts a force on the latter which adds to the force due to the gradient in the electrochemical potential. The additional force on the electrons results in an enhancement of the thermoelectric power. This additional component of the thermoelectric power has been called the phonon-drag component, as distinct from the electronic component which is due to the electrochemical potential alone. In the case of a solid in which the electron density is sufficiently large so that the electron-phonon collisions make a significant contribution to the momentum-dissipation processes for phonons, a rigorous theory of phonon drag is very complicated; we must solve the two coupled transport equations for electrons and phonons or in the

quantum theories solve for the total density matrix of the electron-phonon system. Such is the case for metals. Fortunately we have a much simpler situation: The electron density in a nondegenerate semiconductor is so small that the electron-phonon collisions do not add a significant amount to the lattice thermal resistance, and therefore the relaxation mechanisms for phonons do not depend upon the electron distribution. Moreover, in this case, the electron-phonon collisions conserve crystal momentum so that it is a simple matter to calculate the transfer of momentum from one system to the other. The latter case of a "dilute semiconductor" has been discussed by many authors.<sup>2a,6,25,29,30</sup>

There are two alternative approaches. The first is to calculate the phonon distribution in the presence of a temperature gradient, neglecting the electron-phonon collisions. The phonon distribution thus obtained is then used to calculate the momentum transferred to the electrons in the electron-phonon collision and thus calculate the thermoelectric power. This has been called the  $Q$  approach by Herring.<sup>6</sup> The second alternative is to calculate the electron distribution in the presence of an electric field assuming the temperature gradient to be zero and the phonons in their equilibrium distribution. The momentum transfer due to electron-phonon collisions (with the calculated electron distribution) then constitutes a driving term for the phonon distribution which relaxes by processes other than electron-phonon collisions. From the solution of the phonon transport equation, one obtains the energy flux carried by phonons and hence the phonon-drag component of the Peltier coefficient  $\pi_p$ . This has been called the  $\pi$  approach by Herring.<sup>6</sup>

Either of these methods should give the same end result, although we notice that in the  $Q$  approach we have to solve the electron-transport problem in the presence of an electric field as well as a temperature gradient while in the  $\pi$  approach the temperature gradient is always zero. The incorporation of a spatially varying temperature in the quantum transport theories in the presence of a magnetic field involves some subtle points.<sup>31</sup> We shall avoid these difficulties by using the alternative method of  $\pi$  approach. The calculation is based on Herring's theory.<sup>6,23</sup> The first part of the calculation, that of obtaining the momentum transfer due to the electron-phonon collisions, is done in the quantum theories of transverse magnetoresistance.<sup>32-35</sup> The re-

<sup>29</sup> P. G. Klemens, Proc. Roy. Soc. (London) **A208**, 108 (1951); Australian J. Phys. **7**, 520 (1954); Proc. Phys. Soc. (London) **A68**, 1113 (1955).

<sup>30</sup> V. L. Gurevich and Yu. A. Fisson, Fiz. Tverd. Tela **4**, 530 (1962) [English transl.: Soviet Phys.—Solid State **4**, 385 (1962)].

<sup>31</sup> J. M. Luttinger, Phys. Rev. **135**, A1505 (1964).

<sup>32</sup> E. N. Adams and T. D. Holstein, J. Phys. Chem. Solids **10**, 254 (1959).

<sup>33</sup> R. Kubo and H. Hasegawa, J. Phys. Soc. Japan **14**, 56 (1959).

<sup>34</sup> V. L. Gurevich and Yu. Firsov, Zh. Eksperim. i Teor. Fiz. **40**, 198 (1961) [English transl.: Soviet Phys.—JETP **13**, 137 (1961)].

<sup>35</sup> P. N. Argyres, Phys. Rev. **117**, 315 (1960).

<sup>28</sup> Y. Yafet, Phys. Rev. **115**, 1172 (1959).

maining part of the calculation proceeds as in the zero-field case. We assume that the magnetic field does not affect the phonon-relaxation processes. This is a reasonable assumption, and the measurements of the lattice thermal conductivity in the presence of a magnetic field confirm this expectation. For the sake of completeness we shall derive all the formulas from the beginning.

### A. Phonon Drag for "Free Electrons"

Consider the transport of electrons and phonons in a solid in which a small electric field  $E$  is directed along the  $X$  axis and a strong magnetic field  $B$  is directed along the  $Z$  direction. The steady-state equation for phonons of mode  $q$  can be written as

$$\partial N_q / \partial t \Big|_{\text{electrons}} + \partial N_q / \partial t \Big|_{\text{relaxation}} = 0, \quad (2.1)$$

where the first term is due to the electron-phonon collisions, and the second term is due to phonon collisions other than those on electrons. It is assumed that the phonon distribution  $N_q$  is homogeneous in space coordinates. The second term can be approximated by introducing a relaxation time  $\tau_q$  defined by

$$\partial N_q / \partial t \Big|_{\text{relaxation}} = - (N_q - N_q^0) / \tau_q(\eta), \quad (2.2)$$

where  $N_q^0$  is the thermal equilibrium distribution, and  $\eta$  indicates the state of the media taking part in phonon relaxation. In the case of scattering of phonons from the walls of the specimen,  $\eta$  indicates the size and the surface condition of the sample; and for scattering on impurities,  $\eta$  depends on the number and the nature of impurities. In case of phonon-phonon scattering,  $\eta$  states the distribution of other phonons, i.e.,

$$\tau_q(\eta) \sim \tau_q(N_q', N_q'', \dots).$$

This makes (2.1) a set of coupled equations for different phonon modes. It is next assumed that for the purpose of calculating  $\tau_q(\eta)$  we can regard all phonon modes except  $q$  to have their thermal equilibrium distribution  $N_q^0$ , etc., so that  $\tau(\eta)$  can be replaced by  $\tau_q(T)$  where  $T$  is the lattice temperature. The transport problem for each phonon mode  $q$  can then be discussed separately. The justification for using this "single-mode" relaxation time has been investigated by Herring<sup>6,25</sup> and Carruthers<sup>36</sup> and is seen to be quite good except at extremely low temperatures. The essence of their arguments is that the phonon-drag phonons, i.e., phonons which are shifted significantly from their thermal equilibrium distribution, have wave vectors  $q_p$  much smaller than the wave vector  $q_t$  of thermal phonons. The latter remain in thermal equilibrium because of a much shorter relaxation time. Also, because of their abundance, thermal phonons are the ones which contribute most to the relaxation of low-frequency phonons which justifies the assumption. Since the wave vector of phonon-drag phonons increases continuously with the magnetic field,

<sup>36</sup> P. Carruthers, Rev. Mod. Phys. 33, 92 (1961).

the above criteria also put an upper limit on the magnetic field for which the present calculation is valid. The upper limit on the magnetic field can be obtained from the following argument: In the quantum region, the wavelength of phonons that interact with electrons is approximately equal to the size of the cyclotron orbit which has a radius equal to  $(\hbar c / eB)^{1/2}$  for the lowest orbit. On the other hand, phonons of thermal energy have a wavelength of  $(\hbar S / k_0 T)$ . The above criteria, therefore, demand that

$$(\hbar c / eB)^{1/2} \gg (\hbar S / k_0 T),$$

where  $S$  is the velocity of phonons. This limitation was first pointed out by Gurevich *et al.*<sup>37</sup>

As we assume that  $\tau_q(T)$  is independent of the magnetic field, we have

$$N_q - N_q^0 = \tau_q(T) (\partial N_q / \partial t) \Big|_{\text{elect}}. \quad (2.3)$$

For the time rate of change of  $N_q$  due to electron-phonon collisions, we can write

$$\begin{aligned} \partial N_q / \partial t \Big|_{\text{elect}} = \sum_{\mu\mu'} [W_q^e(\mu \rightarrow \mu') - W_q^a(\mu \rightarrow \mu')] \\ \times f_\mu(1 - f_{\mu'}), \end{aligned} \quad (2.4)$$

where  $W_q^{e(a)}(\mu \rightarrow \mu')$  is the probability of transition for an electron state to go from  $\mu$  to  $\mu'$  through emission (absorption) of a phonon of mode  $q$ ;  $f_\mu$  is the electron-distribution function;  $\mu$  specifies a complete set of quantum numbers including spin which labels the electron states in the presence of external fields. In the one-electron approximation, the Hamiltonian for the electrons can be written as

$$\mathcal{H} = \mathcal{H}_0 + V, \quad (2.5)$$

where

$$\mathcal{H}_0 = (1/2m) \{ p_x^2 + (p_y + \hbar k_B x)^2 + p_z^2 \} + eEx, \quad (2.6)$$

and  $V$  is the interaction potential with phonons, impurities, etc.;  $k_B = (eB/\hbar c)^{1/2}$  has the dimensions of inverse length. We have neglected the energy due to the interaction of electron spin with the magnetic field and assumed an isotropic effective mass for the electrons. The problem of anisotropic mass can be treated<sup>38</sup> but leads to somewhat cumbersome expressions. The eigenfunctions and eigenvalues of  $\mathcal{H}_0$  are given by

$$\psi_{l, k_y, k_z} = \exp\{i(k_y y + k_z z)\} \varphi_l\{k_B(x - x_0)\} \quad (2.7)$$

and

$$\mathcal{E}_{l, k_y, k_z} = \hbar^2 k_z^2 / 2m + (l + \frac{1}{2}) \hbar \omega + eEx_0 \quad (2.8a)$$

$$= \epsilon_{l, k_y, k_z} + eEx_0, \quad (2.8b)$$

where  $\omega$  is the cyclotron frequency  $eB/mc$ ;

$$x_0 = - (1/k_B^2) (k_y + eE/\hbar \omega), \quad (2.9)$$

<sup>37</sup> (a) L. E. Gurevich and G. M. Nedlin, Fiz. Tverd. Tela 3, 2779 (1961) [English transl.: Soviet Phys.—Solid State 3, 2029 (1962)]. (b) T. Ohta, J. Phys. Soc. Japan 18, 909 (1963); 19, 769 (1964).

<sup>38</sup> M. I. Klinger and P. Voroniuk, Zh. Eksperim. i Teor. Fiz. 33, 77 (1957) [English transl.: Soviet Phys.—JETP 6, 1958].

and  $\varphi_l$  are wave functions of a simple harmonic oscillator with energy  $(l+\frac{1}{2})\hbar\omega$ . The energy expression is correct only up to terms linear in the electric field. The two spin states are degenerate, and we have omitted the corresponding quantum number. We assume that the electron density is small enough so that we can use classical statistics, in which case  $(1-f_\mu')\simeq 1$ . Furthermore, in the extreme quantum region,  $\hbar\omega \gg kT$ , all electrons are in the state with  $l=0$ . The magnetic quantum number  $l$  does not change during scattering because of insufficient energy exchange between the electrons and the scatterer; this means that  $l=0$  for both the initial and the final states in (2.4). To calculate scattering in the lowest order,  $f_\mu$  can be taken as the equilibrium distribution with respect to  $\epsilon_\mu$  as defined by (2.8b); we can neglect the electric-field-dependent term in energy<sup>39</sup> for writing  $f_\mu$  if we are interested in calculating  $dN_q/dt]_{\text{elect}}$  correct only up to linear terms in the electric field. Therefore, we can write for the electron distribution in the lowest Landau level

$$f(k_z) = (\gamma/\pi kT)^{1/2} \exp(-\gamma k_z^2/kT), \quad (2.10)$$

where we have written  $\gamma k_z^2$  for  $(\hbar^2/2m)k_z^2$  which is the energy due to electron motion parallel to the magnetic field. In the lowest approximation the transition probability  $W(\mu \rightarrow \mu')$  for any part of perturbation potential is independent of the other part of perturbation. Equation (2.4) is not affected by the presence of impurities, etc. This is very important from the experimental point of view because ionized impurity scattering is almost always present in semiconductors at low temperatures and the present calculation of scattering from a long-range potential in the presence of a magnetic field is of a doubtful nature.<sup>40</sup> From here on, we regard  $V$  to be entirely due to the electron-phonon interactions and expand  $V$  in normal modes of phonon

$$V = \sum_q V_q e^{i\mathbf{q}\cdot\mathbf{r}}. \quad (2.11)$$

Using the Born approximation, the transition probability is given by

$$W_q(\mu \rightarrow \mu') = \frac{2\pi}{\hbar} \left( \frac{N_q+1}{N_q} \right) |V_q|^2 \times |\langle \psi_{\mu'} | e^{\pm i\mathbf{q}\cdot\mathbf{r}} | \psi_\mu \rangle|^2 \delta(\epsilon_\mu - \epsilon_{\mu'} \mp \hbar\omega_q), \quad (2.12)$$

where the upper sign holds for emission of phonon and the lower for the absorption;  $\hbar\omega_q$  is the energy of the phonon exchanged;  $W_q$  depends upon the electric field, and the explicit dependence is contained in the  $\delta$  function of energy. The term  $dN_q/dt]_{\text{elect}}$  can be calculated

by using (2.10) and (2.12). The resulting expression is

$$\begin{aligned} \frac{dN_q}{dt} ]_{\text{elect}} &= -n \left( \frac{\pi}{k_0 T \gamma} \right)^{1/2} \frac{1}{\hbar |q_z|} V_q^2 B_q^f \\ &\times \left[ \frac{eE q_y}{k_B^2 k_0 T} \left\{ N_q \cosh \left( \frac{\hbar\omega_q}{2k_0 T} \right) \right. \right. \\ &+ \frac{1}{2} \exp \left( -\frac{\hbar\omega_q}{2k_0 T} \right) \left. \left. \right\} \right. \\ &+ 2 \left\{ N_q \sinh \left( \frac{\hbar\omega_q}{2k_0 T} \right) - \frac{1}{2} \exp \left( -\frac{\hbar\omega_q}{2k_0 T} \right) \right\} \\ &\left. \times \left[ 1 - \frac{eE q_y}{k_B^2 k_0 T} \frac{\hbar\omega_q}{\gamma q_z^2} \right] \right], \quad (2.13) \end{aligned}$$

where  $B_q^f$  is a dimensionless constant (superscript  $f$  is for free electrons) given by

$$B_q^f = \exp \left( -\frac{\gamma q_z^2}{4k_0 T} \right) \exp \left( -\frac{\hbar^2 \omega_q^2}{4\gamma q_z^2 k_0 T} \right) \times |\langle \varphi_0' | e^{i\mathbf{q}\cdot\mathbf{r}} | \varphi_0 \rangle|^2, \quad (2.14)$$

and  $n$  is the total number of electrons.

Equation (2.13) is correct up to terms linear in the electric field. The second term within the square brackets on the right-hand side of Eq. (2.13) describes the relaxation of phonons to thermal equilibrium due to scattering on electrons. This part of the electron-phonon collisions can be written in terms of a relaxation time, i.e., the collision rate is proportional to  $N_q - N_q^0$ . As was stated in the Introduction, this term gives rise to the "saturation" effect.<sup>6</sup> The first term proportional to the electric field is the "drag" exerted by the drifting electron on a phonon system in thermal equilibrium. The lowest order term of this can be obtained by putting  $N_q = N_q^0$  on the right-hand side. Using (2.3) and (2.13), we can obtain the phonon distribution and the energy flux transported by phonons. Before we do that, we shall consider the effects due to the band structure.

### B. Effect of Nonparabolic Band

So far we have been talking about a hypothetical solid in which the periodic crystal potential is turned off. This model can be used for electrons in a realistic crystal, provided the energy band in which the electrons move is removed far enough on the energy scale from other bands. One has to, in this case, simply replace the free-electron mass by the effective mass of the crystal electrons or, in the more general case of anisotropic energy surfaces, by an effective mass tensor. This approximation is sufficiently accurate for the conduction bands of Ge and Si. But for the valence bands of these materials, and for the valence as well as the conduction

<sup>39</sup> A. H. Kahn and H. P. R. Frederikse, in *Solid State Physics*, edited by F. Seitz and D. Turnbull (Academic Press Inc., New York, 1959), Vol. 9.

<sup>40</sup> A. H. Kahn, *Phys. Rev.* **119**, 1189 (1960).

bands of III-V compound semiconductors, the free-electron model is not appropriate. This is because, owing to the close proximity of the several energy bands, there is a strong interaction between them and the effect of this interaction changes with the magnetic field. Consequently, the energy levels and the wave functions are somewhat different from those obtained for the free electrons. The band-structure effects will be considered in this section. Since we have assumed that all electrons are in the lowest Landau level ( $l=0$ ), we need to know the energy and wave functions of only this level. The spacing between the Landau levels which is affected most<sup>39,41</sup> by the band-structure effects will be of no concern to us.

First of all, we note that the spin-orbit interaction splits the almost spin-degenerate Landau levels by an amount which depends upon the magnitude of the  $g$  factor. The values of the  $g$  factor can be quite large; in  $n$ -InSb, spin splitting of the levels is quite comparable to the Landau level spacing.<sup>42</sup> We assume that there is no scattering of electrons between the spin-split levels. One can then carry out the calculation for each spin state separately and add the final results, taking into account the difference in the Boltzmann occupation probability of each state. The Boltzmann factor, in our case, makes the contribution of the higher of the spin states vanishingly small and we neglect it completely.

Also the curvature of each quantized level  $\gamma$  which relates energy to crystal momentum parallel to the magnetic field is not constant as in the free-electron case but changes with the energy of the quantized level and the magnitude of  $k_z$ . In high magnetic fields, the density of states at  $k_z=0$  is very large,<sup>39</sup> therefore the major contribution to the transport properties comes from states with small  $k_z$ . This makes the transport properties in the quantum region much less sensitive to the change in curvature with  $k_z$  provided the electron gas is non-degenerate. We consider  $\gamma$  to be a function of  $B$  but independent of  $k_z$ . The effects considered so far are small and taken into account in a trivial manner as can be seen from the structure of Eq. (2.13).

Finally we have to consider the change in the wave functions which affects the transition probabilities. As Kane<sup>27</sup> has shown, to get the energy and wave functions away from the band edge it is sufficient, in the case of InSb, to consider the interaction between the conduction band and the triply degenerate valence bands only. In this approximation, in zero field the wave functions of the heavy hole band do not mix with the conduction-band wave functions. Away from the band minima, the conduction-band wave functions have a component of the other two valence bands proportional to  $k$ , the major amount of admixture coming from the light hole band. The mixing of the wave function is due to the  $\mathbf{k}\cdot\mathbf{p}$  term

of the Hamiltonian.<sup>27</sup> In the presence of a magnetic field the momentum operator  $\mathbf{p}$  is replaced by  $\mathbf{p}+e\mathbf{A}/c$ , and in this case the wave functions of the heavy hole bands also enter the conduction-band wave functions.

The problem of finding the electron energy states has been solved independently by Yafet<sup>28</sup> and Roth<sup>43</sup> following the formulation of Luttinger and Kohn.<sup>44</sup> An  $8\times 8$  Hamiltonian matrix is calculated in a representation, the basis of which is formed by the wave functions which diagonalize the Hamiltonian at  $k=0$  in the absence of the magnetic field. The periodic part of these wave functions are symbolically represented by

$$\begin{aligned} & |iS\pm\rangle; \quad (\frac{2}{3})^{1/2}|Z\pm\rangle\mp(\frac{1}{6})^{1/2}|(X\pm iY)\mp\rangle \\ & (1/\sqrt{2})|X\pm iY\rangle\pm\rangle; \quad (\frac{1}{3})^{1/2}|Z\pm\rangle\pm(\frac{2}{3})^{1/2}|(X\pm iY)\mp\rangle. \end{aligned} \quad (2.15)$$

The sign  $\pm$  attached to each symbolic wave function refers to the direction of quantization of spin. The orbitals  $|X\rangle$ ,  $|Y\rangle$ , and  $|Z\rangle$  transform under the symmetry operations of the crystal as coordinates along the cubic axis while  $|S\rangle$  has the symmetry of an  $s$ -type wave function. We denote the eight combinations of (2.15) by  $U_\mu$ , where  $\mu$  goes from one to eight. In the limit  $k=0$ , the combinations  $U_1$  and  $U_2$  correspond to the conduction band,  $U_3$  and  $U_4$  to the light hole band,  $U_5$  and  $U_6$  to the heavy hole band, and the last two to the split-off band. If the magnetic field is directed along one of the cubic axes of the crystal which is chosen as the  $Z$  axis, the eigenvalue equation in the matrix form is given by Eq. (2) of Bowers and Yafet.<sup>45</sup> The eigenfunctions in real space are given by<sup>28</sup>

$$\begin{aligned} \psi_{l,k_y k_z, \pm}^\alpha(\mathbf{r}) = & e^{i(k_y y + k_z z)} \sum_{\mu=1}^8 (-i)^{l-m_j^\mu} \\ & \times C_\mu^\alpha U_\mu(\mathbf{r}) \varphi_{l-m_j^\mu, \pm} \left\{ k_B \left( x - \frac{k_y}{k_B^2} \right) \right\}, \end{aligned} \quad (2.16)$$

where  $\alpha$  refers to the band index and  $C_\mu^\alpha$  are to be obtained by solving Eq. (2) of Ref. 45; the  $\varphi$ 's, as before, are simple harmonic-oscillator wave functions; the  $m_j^\mu$  is the quantum number for angular momentum in the  $Z$  direction. The coefficient  $C_\mu$  is zero for the state for which  $l-m_j^\mu+(-)\frac{1}{2}<0$ . The energy levels are given by the solutions<sup>45</sup> of

$$\begin{aligned} \lambda_{l,\pm}(\lambda_{l,\pm}-E_g)(\lambda_{l,\pm}+\Delta) - P^2[k_z^2 + 2(l+\frac{1}{2})k_B^2] \\ \times [\lambda_{l,\pm} + \frac{2}{3}\Delta] \pm \frac{1}{3}P^2\Delta k_B^2 = 0, \end{aligned} \quad (2.17)$$

where the zero of energy is fixed at the valence-band maximum, in zero field;  $E_g$  is the energy gap;  $P$  is the interband matrix element defined by Kane,<sup>27</sup> and  $\Delta$  is the spin-orbit splitting of the valence band. In the above derivation, terms of the order of  $(3E_g/8P^2m_e)\hbar^2$ , which

<sup>41</sup> See, for example, B. Lax in *Solid State Physics*, edited by F. Seitz and D. Turnbull (Academic Press Inc., New York, 1960), Vol. 11.

<sup>42</sup> G. Bemsli, Phys. Rev. Letters 4, 62 (1959).

<sup>43</sup> L. Roth, B. Lax, and S. Zwerdling, Phys. Rev. 114, 90 (1959).

<sup>44</sup> J. M. Luttinger and W. Kohn, Phys. Rev. 97, 869 (1955).

<sup>45</sup> R. Bowers and Y. Yafet, Phys. Rev. 115, 1165 (1959).

arise from the electron free mass  $m_e$ , have been neglected compared to unity.

We make the further approximation, following Kane,<sup>27</sup> that  $\Delta \gg \lambda$  and obtain the following simpler expressions for the energy and wave functions of the conduction band:

$$\lambda_{l\pm} = \frac{E_g}{2} + \frac{1}{2} \left[ E_g^2 + \frac{8P^2}{3} \{k_z^2 + 2(l + \frac{1}{2})k_B^2\} \mp \frac{4}{3} P^2 k_B^2 \right]^{1/2}, \quad (2.18)$$

$$\psi_{l+} = \frac{(-i)^l}{N_+} \left[ \lambda_l U_1 \varphi_l + \left(\frac{2}{3}\right)^{1/2} P k_z U_3 \varphi_l - i \left(\frac{1}{6}\right)^{1/2} \right. \\ \left. \times \alpha U_4 \varphi_{l+1} + i \left(\frac{1}{2}\right)^{1/2} \alpha U_5 \varphi_{l-1} \right], \quad (2.19)$$

$$\psi_{l-} = \frac{(-i)^l}{N_-} \left[ \lambda_l U_2 \varphi_l + \left(\frac{2}{3}\right)^{1/2} P k_z U_4 \varphi_l + i \left(\frac{1}{6}\right)^{1/2} \right. \\ \left. \times \alpha U_3 \varphi_{l-1} - i \left(\frac{1}{2}\right)^{1/2} \alpha U_6 \varphi_{l+1} \right], \quad (2.20)$$

where  $N_{+,-}$  are the normalization factor, and  $\alpha^2 = P^2 k_B^2 (2l+1)$ . It can be easily seen that as  $B$  goes to zero, the coefficient of  $p$ -wave admixture is the same as given by Eq. (17) of Kane<sup>27</sup> except that  $k_z$  is replaced by  $k$ . If the magnetic field makes an angle  $\theta$  with the cubic axis, the energy values are still given by (2.18) but the wave functions are linear combinations of  $\psi_{l+}$  and  $\psi_{l-}$ .

In accordance with our remarks in the beginning of this section we assume that all electrons occupy the lowest quantized level with energy  $\lambda_0^+$  given by (we omit the + sign on  $\lambda$ )

$$\lambda_0 = \frac{E_g}{2} + \frac{1}{2} \left\{ E_g^2 + \frac{4P^2 k_B^2}{3} + \frac{8P^2 k_z^2}{3} \right\}^{1/2} \\ \simeq \frac{1}{2} E_g + \frac{1}{2} \eta + \gamma k_z^2, \quad (2.21)$$

$$\text{where } \eta = \{E_g^2 + 4P^2 k_B^2/3\}^{1/2} \quad (2.22)$$

$$\text{and } \gamma = \frac{2P^2}{3(E_g^2 + 4P^2 k_B^2/3)^{1/2}}. \quad (2.23)$$

The wave functions are

$$\psi_0^+ = (1/N^+) \left[ \lambda_0 U_1 \varphi_0 + \left(\frac{2}{3}\right)^{1/2} P k_z U_3 \varphi_0 - i \left(\frac{1}{6}\right)^{1/2} P k_B U_4 \varphi_1 \right] \\ \simeq \left[ \frac{\sqrt{2}(\eta + E_g)^{1/2}}{(3\eta + E_g)^{1/2}} U_1 \varphi_0 - i \frac{(\eta - E_g)^{1/2}}{(3\eta + E_g)^{1/2}} U_4 \varphi_1 \right], \quad (2.24)$$

where we have put  $k_z=0$  for the purpose of calculating the coefficients of the wave functions. Since the major contribution to the transport properties comes from states with small  $k_z$ , this assumption is not expected to introduce any serious error. Similarly we have

$$\psi_0^- \simeq \left[ \frac{\sqrt{2}(\eta + E_g)^{1/2}}{(5\eta - E_g)^{1/2}} U_2 \varphi_0 - i \frac{\sqrt{3}(\eta - E_g)^{1/2}}{(5\eta - E_g)^{1/2}} U_6 \varphi_1 \right]. \quad (2.25)$$

Now we assume that, in the presence of an additional

small electric field  $E$  applied transverse to the magnetic field, the energy levels are obtained by adding a term  $eEx_0$  to Eq. (2.21) and the wave functions remain unchanged;  $x_0$  is now given by an expression similar to Eq. (2.9). The electron-phonon scattering rate is calculated as in Sec. IIA. Formally Eq. (2.13) remains valid except that  $\gamma$  is now given by Eq. (2.23) and  $B_q$  has the value for band electrons  $B_q^b$  given by

$$B_q^b = \exp\left(-\frac{\gamma q_z^2}{4k_0 T}\right) \exp\left(-\frac{\hbar^2 \omega_q^2}{4\gamma q_z^2 k_0 T}\right) \\ \times \exp\left(-\frac{q_1^2}{2k_B^2}\right) \left(1 - 2\alpha_p^2 \frac{q_1^2}{2k_B^2} + \alpha_p^4 \frac{q_1^4}{4k_B^4}\right), \quad (2.26)$$

where  $\alpha_p$  is the coefficient of the valence-band admixture. We can now write the phonon transport equation as

$$\frac{N_q - N_q^0}{\tau_q} = -n \left(\frac{\pi}{\gamma k_0 T}\right)^{1/2} \frac{1}{\hbar |q_z|} |V_q|^2 B_q^b \\ \times \left[ \frac{eE q_y}{k_B^2 k_0 T} \left\{ N_q \cosh\left(\frac{\hbar \omega_q}{2k_0 T}\right) \right. \right. \\ \left. \left. + \frac{1}{2} \exp\left(-\frac{\hbar \omega_q}{2k_0 T}\right) \right\} \right. \\ \left. + \left\{ 2(N_q - N_q^0) \sinh\left(\frac{\hbar \omega_q}{2k_0 T}\right) \right\} \right. \\ \left. \times \left[ 1 - \frac{eE q_y}{k_B^2 k_0 T} \frac{\hbar \omega_q}{\gamma q_z^2} \right] \right]. \quad (2.27)$$

Solutions of Eq. (2.27) are obtained by the iteration procedure. The lowest order term is obtained by putting  $N_q = N_q^0$  on the right-hand side. The next correction term gives rise to the saturation effect. We calculate the energy flux due to each term separately.

### C. Thermoelectric Power due to Phonon Drag— No Saturation

Following Herring<sup>6</sup> we can obtain the energy flux  $F$  carried by phonons. Under assumptions similar to that of Ref. 6, we get for  $\mathbf{F}$

$$\mathbf{F} = \sum_q \hbar S^2 \mathbf{q} (N_q - N_q^0), \quad (2.28)$$

where  $S$  is the sound velocity in the crystal and the summation is carried over all modes and all branches of the phonon spectrum. For optical phonons  $S$  is vanishingly small and we can neglect the contribution of optical phonons to  $\mathbf{F}$ . The only nonzero component of  $\mathbf{F}$  is along the  $Y$  direction; other components go to zero

on summation. The Peltier coefficient  $\pi$  is given by<sup>37</sup>

$$\pi_p = (F_u/E)\rho_{yx}, \quad (2.29)$$

where  $\rho_{yx}$  is the element of the magnetoresistance tensor<sup>33</sup>

$$\rho_{yx} = B/nec. \quad (2.30)$$

The thermoelectric power  $Q_p$  is obtained from  $\pi_p$  by using the Kelvin relation:

$$Q_p = -\frac{k_0(\pi k_0 T)^{1/2}}{e\gamma} \frac{1}{(k_0 T)^3} \sum_q S^2 |V_q|^2 \hbar \tau_q(T) B_q^b \frac{q_y^2}{|q_z|} \times \left\{ N_q^0 \cosh\left(\frac{\hbar\omega_q}{2k_0 T}\right) + \frac{1}{2} \exp\left(-\frac{\hbar\omega_q}{2k_0 T}\right) \right\}. \quad (2.31)$$

The form of  $V_q$  to be used depends upon the mode of electron coupling to acoustic phonons. For scattering due to the deformation potential we have

$$V_q = \eta_D (\hbar q / 2\delta S)^{1/2},$$

where  $\eta_D$  is the deformation potential constant and  $\delta$  is the density of the crystal. For piezoelectric mode of scattering we have

$$V_q = \eta_P (\hbar / 2\delta S q)^{1/2},$$

where  $\eta_P$  is the coupling constant of the dimensions of force. Since the two types of scattering arise from the same source, there may be coherence between them. Therefore we put

$$|V_q|^2 = (\hbar / 2\delta S) \{ \eta_D^2 q + 2\eta_P \eta_D \cos\beta + \eta_P^2 / q \}, \quad (2.32)$$

where  $\beta$  is the phase correlation between two types of scattering.

#### D. Saturation Effect

In the above derivation [Eq. (2.31)] we have assumed that the relaxation time of phonons  $\tau_q$  is determined by phonon-phonon collisions or phonon collisions on the walls of the specimen; in particular, we have neglected the influence of electron-phonon collisions on  $\tau_q$ . Formally this approximation is introduced by replacing  $N_q$  on the right-hand side of Eq. (2.27) by  $N_q^0$  which makes the second term within the square brackets of that equation equal zero. Obviously, this assumption is valid for vanishingly small density of the charge carriers. If the density of charge carriers is large enough the electron-phonon scattering decreases the phonon relaxation time and hence the phonon drag  $Q_p$ . This decrease in  $Q_p$  due to a finite density of charge carriers has been called the "saturation effect" by Herring. The density of charge carriers for which the saturation effect becomes significant will depend upon the relaxation time due to phonon-phonon scattering and the boundary scattering of phonons; the longer the relaxation time, the smaller the value of  $n$  for which the saturation effect shows up. The correction due to the

saturation effect is therefore larger at lower temperatures. Moreover, since the electron-phonon scattering rate in the quantum region depends upon the magnetic field, the correction due to the saturation effect may change with the field. If the phonon relaxation time is independent of  $q$ , for example in the case of boundary scattering of phonons, the saturation effect increases with the magnetic field. The correction to  $Q_p$  arises from the second-order term in the solution of Eq. (2.27). In this section we shall calculate this correction. The correction to the phonon spectrum  $\Delta(N - N_q^0)$  is given by

$$\begin{aligned} \Delta(N_q - N_q^0) &= -2 \sinh\left(\frac{\hbar\omega_q}{2k_0 T}\right) (N_q - N_q^0) \\ &\times n\left(\frac{\pi}{k_0 T \gamma}\right)^{1/2} \frac{\tau_q}{\hbar |q_z|} |V_q|^2 B_q^b \\ &= -2 \sinh\left(\frac{\hbar\omega_q}{2k_0 T}\right) n^2 \left(\frac{\pi}{\gamma K_0 T}\right) \\ &\times \frac{\tau_q^2}{\hbar^2 q_z^2} |V_q|^4 B_q^2 \frac{eE q_y}{k_B^2 k_0 T} \\ &\times \left[ N_q^0 \cosh\left(\frac{\hbar\omega_q}{2k_0 T}\right) + \frac{1}{2} \exp\left(-\frac{\hbar\omega_q}{2k_0 T}\right) \right]. \end{aligned} \quad (2.33)$$

Following the steps of Eqs. (2.28) to (2.31) we obtain

$$\Delta Q_s \simeq -\frac{k_0}{e} \left[ n\left(\frac{\pi}{\gamma k_0 T}\right) \left(\frac{1}{k_0 T}\right)^2 \sum_q S^2 \frac{q_y^2}{q_z^2} |V_q|^4 B_q^2 \right], \quad (2.34)$$

where  $\Delta Q_s$  is the correction to  $Q_p$  due to the saturation effect.

The phonon-drag thermoelectric power can be obtained by integrating Eqs. (2.31) and (2.34). We have taken into account the inelasticity of electron-phonon collision which also removes the divergence pointed out by Kubo<sup>33</sup> and Adams and Holstein<sup>32</sup> in the corresponding case of magnetoresistance. Results similar to Eq. (2.31) have been obtained by other authors.<sup>37</sup> These authors have not considered the band-structure effects nor the "saturation effect." The correction due to the saturation effect changes with the magnetic field; it can either decrease or increase with the magnetic field, depending upon how fast the relaxation time of phonons changes with the wave vector  $q$ . The percentage correction increases with the field if  $|V_q|^2 \tau_q$  is an increasing function of  $q$  and vice versa. We also like to point out again that in the quantum region the phonon drag  $Q$  is independent of electron scattering other than that on acoustic phonons. This result holds only in the case of transverse fields and arises because of the peculiar fact that the current flow in the direction of the electric field



is caused by scattering processes themselves. From our procedure it is clear that we have calculated the so-called "isothermal" coefficient of thermoelectric power, i.e., the temperature gradient is zero except in the direction in which the electric field is measured. On the other hand, the arrangement of the experiments is such that it measured the adiabatic coefficient. The difference between the two types of coefficients is expected to be negligible in a solid where thermal conduction is mostly due to lattice waves.

### III. ELECTRONIC PART OF $Q$

We gave a rather detailed discussion of the electronic part of  $Q$  in our earlier paper<sup>1</sup> where we also discussed the discrepancy between our calculations and those of Ref. 5. After we submitted our paper<sup>1</sup> for publication, we became aware of some recent work<sup>46,47</sup> in which the same problem has been discussed using slightly different approaches. Obratsov<sup>47</sup> has discussed the corrections to the thermomagnetic coefficients that arise from the diamagnetism of the conduction electrons in the quantum region. He has pointed out, as we also did,<sup>1</sup> the neglect of the electrostatic part of the energy in the calculations of Anselm and Askerov.<sup>5</sup> According to him, only the electrostatic part of the energy is affected by the corrections due to diamagnetism. It is rather difficult to see how far and in what manner the corrections pointed out by him apply to our calculation. Zyryanov and Silin<sup>46</sup> have criticized the  $\pi$  approach in calculating the thermomagnetic coefficients in the quantum region. They point out that Einstein's relation is not valid in the collisionless transport problem in the quantum region. It seems to us that their criticism should be directed to the use of Einstein's relation for calculating the Peltier coefficient  $\pi$  rather than the use of the  $\pi$  approach itself in the quantum region. There is not enough evidence that the Onsager's relation breaks down in the quantum region and the  $\pi$  approach merely uses one of these relations. In our calculation, for example, we have used the Kelvin relation but not the Einstein's relation. A detailed discussion of these works is beyond the scope of the present work.

Although our calculation is elementary and lacks mathematical rigor, we believe it is nearer the truth than, for example, the work of Anselm *et al.*<sup>5</sup> A reason for this conviction, among other things, is the experimental evidence that we presented in Ref. 1, especially in Fig. 5 of that paper. It is not likely that the difference between the end results of our calculation and that of a more careful solution of the problem will be so large as to change the results of this analysis. At worst, it may mean corrections of the order of few percent in the numerical values of the constants obtained. Therefore, we

have calculated the electronic part of  $Q$  as in Ref. 1 except that we have made corrections to account for the nonparabolic band. This has been done by using the energy spectrum given by Eq. (2.18) instead of Eq. (A3) of Ref. 1. The change in the electronic part of  $Q$  in the quantum region beyond its limiting value in the classical high-field region is given by

$$\Delta Q_e^c = Q_e(B) - Q_e^{\text{limiting}}$$

$$= \frac{k}{e} \left[ \ln \frac{\sum_{l=0}^{\infty} x_l^{1/2} \exp(-x_l)}{\sum_{l=0}^{\infty} x_l^{3/2} \exp(-x_l)} + \frac{\sum_{l=0}^{\infty} x_l^{3/2} \exp(-x_l)}{\sum_{l=0}^{\infty} x_l^{1/2} \exp(-x_l)} - 1 + \frac{1}{2} \ln \left( \frac{8P^4 k_B^4}{9E_g^3 kT} \right) + \ln \frac{n_0}{n_B} \right], \quad (3.1)$$

where

$$x_l = \frac{\frac{1}{2} \{ E_g^2 + (8P^2 k_B^2 / 3) (l + \frac{1}{2}) \}^{1/2}}{kT}, \quad (3.2)$$

and where  $n_0$  and  $n_B$  are the charge carrier densities in zero field and magnetic field  $B$ , respectively. This procedure takes into account the spin splitting of the Landau levels as well as the change in the effective mass parallel to the magnetic field, with the quantum number  $l$  and the field  $B$ . The dependence of  $\gamma$  on  $k_z$  has been neglected.

### IV. EXPERIMENT

Most of the details of the experiment were given in Ref. 1. Here we want to make some additional remarks to supplement those in our earlier paper. The experiment in high field measured only the change in the Seebeck voltage for a constant heat input to the sample as the magnetic field was increased. There is enough reason to believe<sup>1</sup> that the mean temperature of the sample as well as the temperature gradient did not change with the field. The temperature gradient was determined indirectly<sup>9</sup> by comparing the observed Seebeck voltage with the calculated value of  $Q$  in the classical high-field region where  $Q$  takes a limiting value. For such fields, the electronic part of  $Q$  does not depend upon the mechanism of electron scattering and can be calculated accurately,<sup>1</sup> knowing the electron density. The small contribution due to phonon drag in the classical region was replaced by  $Q_p$  measured on sample 581 in zero field.

Figure 1 shows the limiting value in classical high fields of the total thermoelectric power thus calculated for sample 808. The dotted part of the curve gives the electronic contribution;  $Q_p$  is the difference between the two curves and is seen to be small. The neglect of increase in  $Q_p$  in the classical region implies that the temperature gradient thus determined was slightly over-

<sup>46</sup> P. S. Zyryanov and V. P. Silin, Zh. Eksperim. i Teor. Fiz. **46**, 537 (1963) [English transl.: Soviet Phys.—JETP **19**, 366 (1964)].

<sup>47</sup> Yu. N. Obratsov, Fiz. Tverd. Tela **6**, 414 (1964) [English transl.: Soviet Phys.—Solid State **6**, 331 (1964)].

TABLE I. The measured values of the increase in thermoelectric power  $\Delta Q^e$  over the classical limiting value  $Q_{\text{limit}}$ . We have  $\Delta Q^e = Q(B) - Q_{\text{limit}}$ . The calculated values of the electronic component of  $\Delta Q^e$  are given as  $\Delta Q_e^e$ . The difference between the two is the phonon-drag component  $\Delta Q_p^e$ . The numbers are in  $\mu\text{V}/\text{deg}$ .

$T$ ( $^{\circ}\text{K}$ ) \ / $B$ (kG)		10	20	30	40	50	60	70	80	90	100
6.5	$\Delta Q^e$	357.3	1518.0	3242.0	5139.0	7022.0	8477.0	9179.0	9682.0	9857.0	9751.0
	$\Delta Q_e^e$	83.8	146.0	181.0	207.0	226.3	242.0	254.8	266.5	277.5	289.2
7.7	$\Delta Q^e$	316.3	1281.0	2709.0	4288.0	5939.0	7380.0	8488.0	9416.0	10102.0	10539.0
	$\Delta Q_e^e$	71.2	129.9	165.9	191.2	211.4	227.4	241.4	253.2	264.1	273.1
8.8	$\Delta Q^e$	278.5	1101.8	2286.6	3622.9	5035.0	6307.8	7326.7	8245.4	9075.7	9740.3
	$\Delta Q_e^e$	61.5	118.2	153.6	179.5	200.2	215.8	230.0	241.6	252.7	261.9
10.1	$\Delta Q^e$	291.0	1034.7	2096.4	3291.6	4564.9	5689.5	6658.1	7551.9	8362.4	9051.8
	$\Delta Q_e^e$	51.8	107.0	142.4	168.0	188.1	204.5	218.3	230.0	240.9	250.6
11.9	$\Delta Q^e$	237.4	830.1	1644.7	2529.0	3483.8	4331.3	5099.5	5764.2	6395.3	6954.5
	$\Delta Q_e^e$	42.0	94.1	128.3	154.3	174.3	190.6	204.4	216.2	227.4	236.9
17.7	$\Delta Q^e$	154.0	580.1	1166.2	1784.8	2441.9	3052.8	3624.9	4019.5	4547.2	4812.8
	$\Delta Q_e^e$	24.6	62.1	94.8	119.7	139.7	155.3	169.2	181.7	192.5	202.2
20.4	$\Delta Q^e$	118.5	441.2	875.4	1329.3	1805.5	2225.8	2598.7	2923.4	3225.9	3480.1
	$\Delta Q_e^e$	20.3	52.8	82.9	107.2	127.0	143.2	156.9	169.3	180.1	189.9
24.0	$\Delta Q^e$	78.0	348.8	678.5	1026.2	1383.7	1692.0	1957.1	2196.5	2401.2	2586.2
	$\Delta Q_e^e$	16.8	43.3	70.5	93.6	113.2	129.5	143.0	155.5	166.6	175.6
27.1	$\Delta Q^e$	70.8	252.0	480.5	723.2	962.8	1173.4	1348.2	1511.8	1661.1	1793.0
	$\Delta Q_e^e$	14.9	37.6	62.1	84.2	103.1	119.3	132.8	144.9	156.1	165.3
30.2	$\Delta Q^e$	39.7	157.0	306.6	459.0	610.0	742.9	853.9	954.9	1046.3	1128.1
	$\Delta Q_e^e$	13.6	26.2	54.5	76.6	94.7	110.5	124.0	135.9	146.8	156.1
33.4	$\Delta Q^e$	28.8	110.7	215.6	322.5	427.4	519.8	597.3	666.9	731.8	786.9
	$\Delta Q_e^e$	12.9	29.5	49.6	69.3	86.9	102.0	115.6	127.5	138.1	147.3
37.5	$\Delta Q^e$	18.3	75.3	147.8	221.1	292.8	356.0	409.1	457.3	502.1	556.1
	$\Delta Q_e^e$	12.3	26.1	43.6	61.5	77.8	92.8	105.9	117.6	128.0	137.5
43	$\Delta Q^e$	11.7	49.6	98.3	147.4	196.2	239.3	275.3	308.7	339.9	368.1
	$\Delta Q_e^e$	12.3	20.3	37.3	52.6	67.7	81.1	94.2	105.7	116.0	126.0
54	$\Delta Q^e$	7.6	33.2	67.7	102.7	137.9	169.3	195.7	219.9	242.9	266.1
	$\Delta Q_e^e$	12.9	20.0	30.3	42.1	54.3	66.1	77.5	88.1	97.8	106.9
82	$\Delta Q^e$	1.3	15.8	30.1	55.4	76.9	95.9	111.1	125.6	138.9	151.9
	$\Delta Q_e^e$	16.5	19.9	24.9	31.3	38.5	46.0	53.8	61.6	69.2	76.6

estimated as to its actual value. The error in  $\Delta T$  due to this is, at the worst, less than 10% as can be roughly determined from the magnitudes of  $Q_e$  and  $Q_p$  in the classical region. Obviously a better procedure would have been to measure  $Q$  directly, at least in the classical region. Unfortunately, absolute measurements of  $Q$  could not be made on the samples which were used for high-field measurements. The numerical results in the analysis are obtained from the data for sample 808

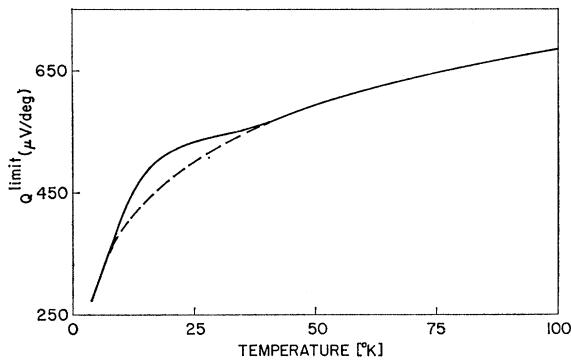


FIG. 1. The calculated values of the thermoelectric power in the classical saturation region for sample 808. The electronic part (dashed curve) which is independent of electron scattering in this region is calculated from the known values of the electron density. The phonon-drag part which makes a small correction between 10 and 30°K is replaced by the measured values of  $Q_p$  in zero field. The solid curve is the sum of the two contributions.

which, of all the samples, had the highest electron mobility, the least density of charge carriers and the highest value for the electronic part of  $Q$ . Thus the errors due to the above-cited reasons were the smallest. Sample 801 was broken during the experiment before we could collect all the high-field data on that sample. The difference between the measurements on these two samples is small. The increase,  $\Delta Q^e [= Q(B) - Q(\text{limit})]$ , of the total thermoelectric power in the quantum region over its classical limiting value is given in Table I for sample 808 for a few selected values of the magnetic field. The electronic part of  $\Delta Q^e$  calculated from Eq. (3.1) is also given in the same table as  $\Delta Q_e^e$ . The first two terms of (3.1) were evaluated numerically terminating the summation over  $l$  at  $l=20$ . The phonon-drag part of  $\Delta Q^e$  is obtained by subtracting the electronic part from the measured value. Figure 2 shows the typical values of the various quantities at 43 and 8.8°K which are, respectively, in the upper and lower range of temperatures. The results obtained in this paper are obtained by comparing  $\Delta Q_p^e$  with the theoretical phonon drag  $Q$  given by Eqs. (2.31) and (2.34).

## V. ELECTRON-PHONON INTERACTION

Besides the information about the band structure, the phonon drag  $Q$  involves two unknown quantities, viz., phonon-relaxation time  $\tau_q$  and the constants of electron-phonon interactions. The constants of the

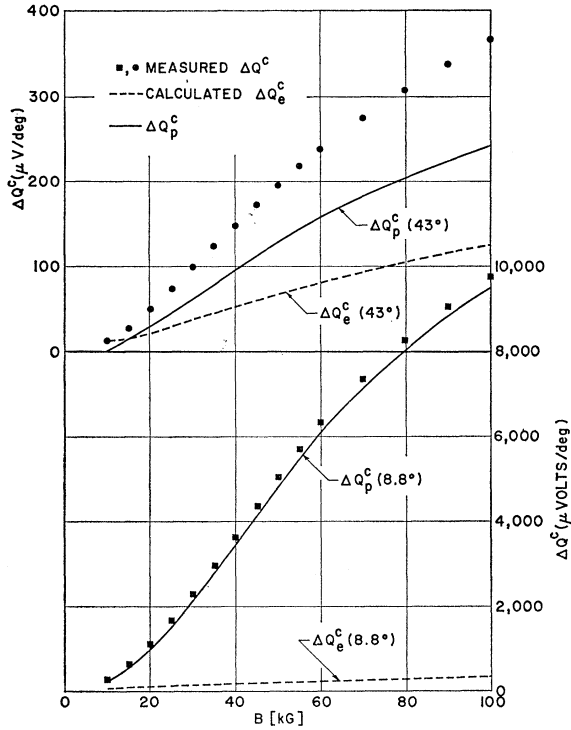


FIG. 2. Some typical values of  $\Delta Q^c$ , the increase in the thermoelectric power in the quantum region over its limiting value in classical high fields. The calculated values of the electronic part of  $\Delta Q^c$  are shown by the dotted curve. The solid curve shows the phonon-drag part of  $\Delta Q^c$  obtained by subtracting the electronic component from the total measured values.

band structure are fairly well established. At the low-temperature end of the range of our measurements  $T \lesssim 20^\circ\text{K}$ , the phonon-drag phonons have a very long relaxation times due to collision with other phonons. The resultant relaxation length is of the order of several cm. If, as is usually the case, the experimental sample has a cross-sectional dimension about 1 mm, these phonons collide much more frequently with the walls of the specimen than with other phonons. The phonon-relaxation time due to boundary scattering is determined by the dimensions of the sample and the velocity of sound; it is independent of  $q$  and  $T$ . For the boundary-scattering relaxation time  $\tau_b$ , we use

$$\tau_b = b/S, \quad (5.1)$$

where  $b$  is the width of the sample perpendicular to the magnetic field and the temperature gradient. To get information about the electron-phonon interaction, we assume that below  $12^\circ\text{K}$ , phonon-phonon collisions are completely negligible and the phonon-relaxation time is given by the known quantity of Eq. (5.1).

#### A. Deformation Potential versus Piezoelectric Mode

The electron-phonon interaction is determined essentially by two constants; the deformation-potential

constant  $\eta_D$ , and another constant  $\eta_P$  which determines the piezoelectric mode of scattering. The first question that we want to investigate is the relative magnitudes of the two types of scattering. This question can be settled by the magnetic-field dependence of  $\Delta Q_p^c$  as can be seen by an inspection of the results obtained after integrating the expressions of (2.31) with the phonon-relaxation time given by (5.1). For a first estimate, we neglect the effects due to the nonparabolic nature of the band. The resulting theoretical expression is

$$Q_p = \text{const}(2k_B^2)^2$$

$$\times \left[ \eta_D^2 I_2 + \left( \frac{\pi}{2k_B^2} \right)^{1/2} I_{3/2} \cos\beta \times \eta_D \eta_P + \frac{I_1}{2k_B^2} \eta_P^2 \right], \quad (5.2)$$

where

$$\text{const} = \frac{k_0}{e} \left( \frac{1}{2\pi} \right)^2 \left( \frac{\pi k_0 T}{\gamma} \right)^{1/2} \left( \frac{\hbar \tau_b}{2\delta} \right) \left( \frac{1}{k_0 T} \right)^2 \quad (5.3)$$

$$I_n = \int_0^1 \frac{(1-x^2)}{x} \exp(-\nu/x^2) \frac{1}{(\alpha x^2 + 1)^n} dx, \quad (5.4)$$

$$\nu = \hbar^2 L^2 / 4\gamma k T; \quad \alpha = [(\gamma k_B^2) / (2k_0 T)] - 1,$$

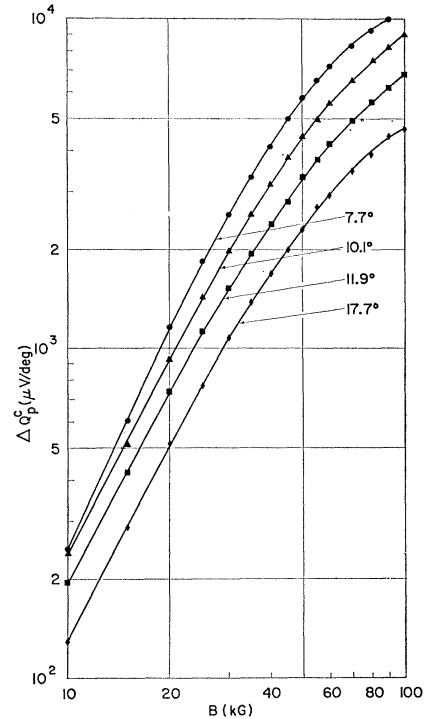


FIG. 3. Measured values of the phonon-drag component of the thermoelectric power in the quantum region plotted as a function of magnetic field for various temperatures. The range of temperatures is where the mean free path of phonon-drag phonons is determined by the size of the experimental specimen. The quadratic variation of  $\Delta Q_p^c$  with  $B$  indicates the piezoelectric mode of electron scattering is unimportant as compared to scattering via deformation potential.

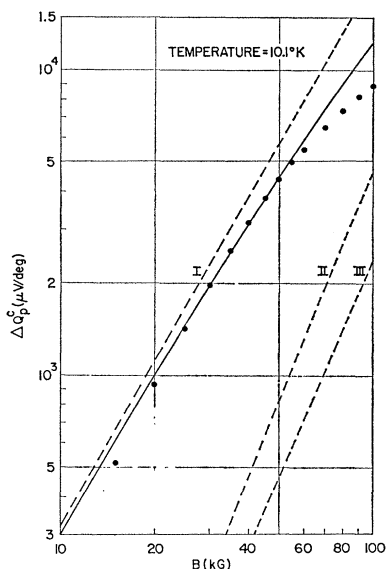


FIG. 4. The comparison of the calculated values of phonon-drag thermoelectric power for boundary-scattered phonons with the measured values. The curve marked I shows the calculated values neglecting the admixture of valence-band wave functions and the saturation effect. The curve marked II is the correction, to be subtracted, due to the admixture of valence-band wave functions. The correction due to the saturation effect also to be subtracted is given by curve III. The solid line gives the sum of the three contributions. The deformation-potential constant  $\eta_D$  which is the only unknown of the theory is adjusted to match the experimental values shown by dots.

and  $I$ 's are numbers of the same order which have only a very weak dependence on the magnetic field and the temperature. If  $\eta_D=0$ , then  $Q_p$  varies linearly with the magnetic field; on the other hand, if  $\eta_P=0$ , then  $Q_p$  varies quadratically with  $B$ . This is in accord with the similar results obtained by Adams and Holstein<sup>32</sup> for transverse magnetoresistance. If the two types of scattering are comparable, the exponent of  $B$  will change with the field, starting with a value 1 and approaching a value 2 for very high fields, i.e., the  $Q_p$ -versus- $B$  curve is bent upwards. The experimental results for a set of temperatures are shown in Fig. 3. The selected range of temperatures is low enough for phonon-phonon scattering to be negligible, and also the conditions for the extreme quantum region are satisfied before the effects due to nonparabolic band become important. On the other hand, the temperature is high enough so that the use of classical statistics for the electron gas is valid. The magnetic field dependence of  $\Delta Q_p^e$  changes with the field; the curve bends down as the field is increased. The observed change in curvature has the opposite sign from what may be considered as due to the mixing of deformation potential- and piezoelectric-type scattering. In fact, the change in curvature arises from the nonparabolicity of the band.

With the exception of 7.7°K curve, the thermoelectric power increases almost quadratically with the field between 10 and 30 kG where the corrections due

to the nonparabolicity of the band are small. At 7.7°K the thermoelectric power falls off even more rapidly than  $B^2$  at the lower end of the magnetic-field range. At still lower temperature (6.5°K) the departure from the quadratic law is even greater.

There may be two reasons for the breakdown of the quadratic law; first, the approach towards the degeneracy temperature and second, the effect of ionized impurity scattering. In quantum regions the degeneracy condition of the electron density changes with the magnetic field because of a change in the density of states. Therefore, under the conditions of mixed statistics that we have at low temperatures the behavior of the thermoelectric power will be different from the quadratic field dependence of the nondegenerate electron gas. Also the ionized impurity scattering reduces the phonon drag to almost zero in the classical region, while in the extreme quantum region the phonon drag, as we pointed out earlier, is expected to be unaltered by the presence of ionized impurity scattering. A smooth transition of these conditions will increase the exponent of  $B$  in  $Q_p$ -versus- $B$  curve. The data of Fig. 2 nevertheless suggest that the piezoelectric mode of scattering is negligible and that most of electron-phonon scattering occurs through the deformation potential. These conclusions find further confirmation from a detailed comparison with theory of the above data and also the results at higher temperatures. Therefore, for the remaining part of this paper we equate  $\eta_P$  to zero.

## B. Size of Deformation-Potential Constant

Once we accept that the piezoelectric mode of scattering is negligible and that the phonon-relaxation time is given by (5.1), the only unknown of the theory is the deformation-potential constant. The value of  $\eta_D$  can therefore be determined from the magnitude of  $\Delta Q_p^e$  in the boundary scattering range of phonons. The theoretical values are obtained by a numerical integration of Eq. (2.31). The correction due to the saturation effect is calculated from Eq. (2.34). The following numerical constants related to InSb are used:

$$S = 3.7 \times 10^8 \text{ cm/sec,}$$

$$\delta = 5.79 \text{ g/cc,}$$

$$E_g = 0.23 \text{ eV,}$$

$$P = 0.44 \text{ a.u.}$$

Figure 4 shows the relative magnitude of the different terms of the theory calculated for  $T=10.1^\circ\text{K}$  assuming  $\eta_P=0$ . The dotted curve marked I is the  $Q_p$  of a free-electron gas with an effective mass which changes slowly with the magnetic field according to Eq. (2.23). It is calculated from Eq. (2.31) after replacing  $B_q^b$  by its free-electron value  $B_q^f$  as given by Eq. (2.14). The curve marked II is the correction to be subtracted when the band-structure effects are considered. This is also calculated from Eq. (2.31) replacing  $B_q^b$  [Eq. (2.26)]

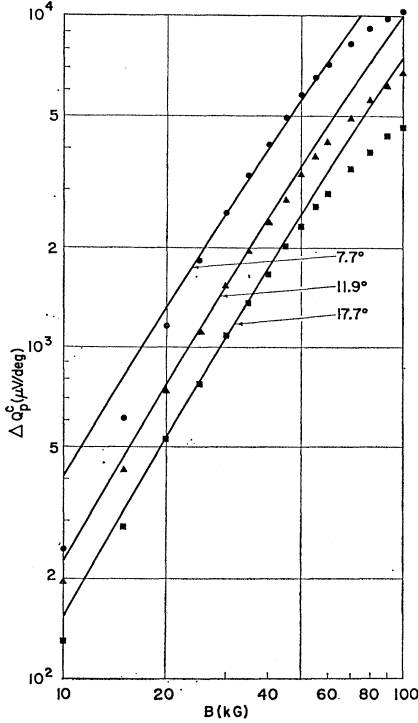


FIG. 5. The comparison of the calculated values of phonon-drag thermoelectric power with the measured values. The deformation-potential constant  $\eta_D$  is adjusted to match the experimental points. The values of  $\eta_D$  thus obtained are listed in Table II.

by the difference  $(B_q^b - B_q^f)$ . The correction is small and negligible at low fields as may be expected for an electron density of  $3 \times 10^{13}/\text{cc}$  at  $10.1^\circ\text{K}$  in the classical region. The percentage correction increases with the field as the valence-band admixture increases and becomes  $\sim 24\%$  at  $100 \text{ kG}$ . The term due to the saturation effect also to be subtracted is marked as III. This is calculated from Eq. (2.34). For calculating this term we have neglected the band-structure effects, i.e., replaced  $B_q^b$  by its free-electron value  $B_q^f$ . The saturation term also increases from a value of less than  $3\%$  at  $10 \text{ kG}$  to more than  $12\%$  at  $100 \text{ kG}$ . The solid curve is the algebraic sum of all the contributions. The experimental data are marked by encircled points.

Figure 5 shows the comparison of the experimental data at other temperatures in the boundary-scattering range of phonons to the theoretical values corresponding to the solid curve of Fig. 4. The value of  $\eta_D$  is adjusted in each case to normalize the theoretical curve to the experimental value at  $30 \text{ kG}$ . It is seen from Figs. 4 and 5 that between  $25$  and  $60 \text{ kG}$  the experimental data are in fair agreement with the calculated values, assuming no piezoelectric scattering. The good agreement obtained within these limits of the magnetic field is spoiled and the disagreement that already exists outside these limits is considerably worsened if a finite amount of piezoelectric scattering is introduced. This further confirms our initial assumption of  $\eta_P$  being zero. Below

$25$  and above  $60 \text{ kG}$ , the experimental values fall below the calculated curve. The disagreement at the lower end of the magnetic-field range may be, as explained earlier, due to the increasing influence of ionized impurity scattering as the field is decreased from a high value. The reason for disagreement at high fields is not clear, but it probably arises due to the limitation of the above rather simplified theory. We shall postpone the discussion of this point to Sec. VII and confine our attention, for the moment, to data between  $25$  and  $60 \text{ kG}$  where good agreement is obtained.

The values of the deformation-potential constant  $\eta_D$  obtained from the data at different temperatures are listed in Table II. The different values agree with each other within  $5\%$ . Owing to some experimental error the measured values of  $\Delta Q_p^c$  at  $11.9^\circ\text{K}$  are too low (as is seen in Fig. 5), which explains the rather large deviation of  $\eta_D$  at  $11.9^\circ\text{K}$ . From Table II we get an average value of  $\eta_D = 8.25 \text{ eV}$ .

## VI. PHONON RELAXATION TIME

Next we turn our attention to the data at higher temperatures where the relaxation time of phonons is determined by phonon-phonon collisions. Since the piezoelectric scattering is negligible and the electron-energy surfaces are isotropic in momentum space, the transverse phonons are not expected to interact with the electrons. Of course, we have assumed that in the long-wavelength limit, phonon branches can be labeled as purely longitudinal or purely transverse. So the information that we get about the phonon relaxation time relates only to the longitudinal phonons. What we wish to find is the frequency and temperature dependence of the relaxation time and possibly its absolute magnitude. Guided by Herring's expressions for the relaxation time of long-wavelength phonons due to collision with thermal phonons, we assume a relaxation time of the form

$$\tau_q(T) = A/q^m T^r. \quad (6.1)$$

Using (6.1) in Eq. (2.31) and integrating, we get the thermoelectric power in the phonon-phonon scattering range:

$$\Delta Q_p^c = \text{const}(\eta_D^2 A/T^r)(2k_B^2)^{2-m/2} I_{3/2}, \quad (6.2)$$

TABLE II. The values of the deformation-potential constant  $\eta_D$  obtained by matching the calculated values of  $\Delta Q_p^c$  to the measured values in the boundary-scattering region of phonons at different temperatures. A good match between the two values is obtained for magnetic fields between  $25$  and  $60 \text{ kG}$ .

$T$ ( $^\circ\text{K}$ )	$\eta_D$ (eV)
6.5	8.59
7.7	8.43
8.8	8.15
10.1	8.31
11.9	7.90
17.7	8.12
Average $\eta_D = 8.25 \text{ eV}$	

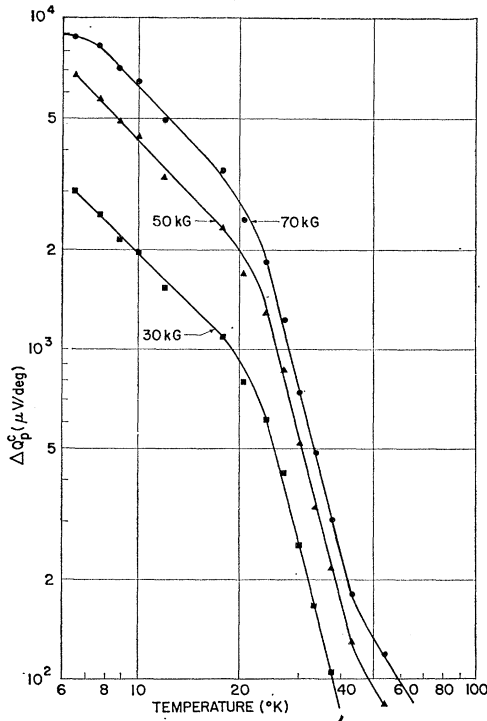


FIG. 6. The phonon-drag thermoelectric power for fixed magnetic field in the quantum region plotted as a function of temperature. The straight line drawn through the data points between 25 and 45°K has a slope of 4.46 indicating that the relaxation time of phonons varies as  $T^{-3.0}$ .

where the constant is again given by (5.3) and  $I_{3/2}$  is an integral of the form (5.4). Neglecting the weak temperature dependence of  $I_{3/2}$ , we observe that, for a fixed magnetic field,  $\Delta Q_p^e \sim T^{-(r+3/2)}$ . The measured values of  $\Delta Q_p^e$  for fixed values of the magnetic field are plotted against temperature in Fig. 6. A straight line with a slope of 4.46 can be drawn through the data between 27 and 43°K, suggesting a value of 3.0 for  $r$ . Above 43°K, deviations from the straight line are observed which are expected as the temperature approaches the Debye temperature ( $\sim 205^\circ\text{K}$ ).

Figure 7 shows the comparison of the measured values of  $\Delta Q_p^e$  at  $T=33.4^\circ\text{K}$  with two different calculated curves. We have used  $m$  equal to one and two to calculate curves marked I and II, respectively. Both the curves are normalized to the measured value at 35 kG. The band-structure effects and the saturation effect are taken into account as in Sec. V. It is clear that a value of  $m=1$  gives a much better fit to the data in the intermediate field range. Deviations are observed in both low-field and high-field ranges. Deviations at low fields are probably due to the effect of ionized impurity scattering as explained in Sec. V and also due to the reduced accuracy of the data because of its small value.

Using the value of  $\eta_D$  obtained in Sec. V, we can find the constant  $A$  of Eq. (6.1) where  $r=3$  and  $m=1$ . The values of  $A$  obtained by normalizing the calculated

TABLE III. The values of constant  $A$  [Eq. (6.1)] obtained by matching the calculated values of  $\Delta Q_p^e$  using  $\eta_D=8.25$  eV to the measured values in phonon-phonon scattering region.

$T$ (°K)	$A$
30.2	$4.48 \times 10^8$
33.4	$4.33 \times 10^8$
37.5	$4.32 \times 10^8$
43	$4.37 \times 10^8$
Average $4.37 \times 10^8$	

value to the experimental data at different temperatures are listed in Table III. The different values are again consistent with each other within about 5%.

Incidentally, we also find that if it is assumed that the piezoelectric scattering of electrons is the dominant mode of scattering, we have to assume a negative value of  $m$  to fit the experimental data. This implies a phonon-relaxation time increasing with the wave vector of phonons, which is not likely. The data again confirms the absence of any appreciable amount of piezoelectric scattering.

## VII. DISCUSSION

To summarize, we have found that the deformation-potential type of scattering dominates the electron-phonon interaction in  $n$ -InSb for  $T \geq 6^\circ\text{K}$ . The value of 8.25 eV is obtained for the deformation-potential constant. The relaxation time of long-wavelength longitudinal-acoustical phonons for  $T \leq 40^\circ\text{K}$  is given by

$$\tau_q(T) = (4.4 \times 10^8) / q T^3 \text{ sec},$$

where  $q$  is in  $\text{cm}^{-1}$  and  $T$  in degrees Kelvin.

The value of the deformation-potential constant obtained from this experiment is close to Ehrenreich's estimate of 7.2 eV for the same constant. However, our value is by a factor of 4 smaller than the value obtained by Haga and Kimura from the analysis of free-electron infrared absorption. The phonon-drag experiment can-

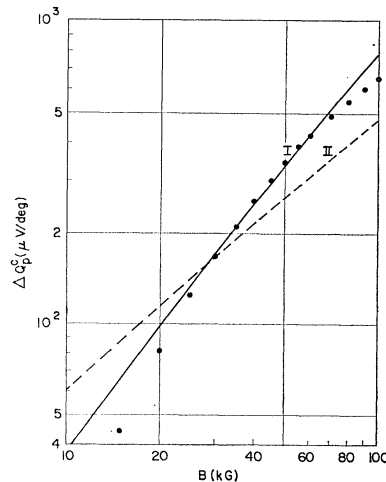


FIG. 7. The comparison of the measured values of the phonon-drag thermoelectric power with the calculated values. The solid curve marked I is calculated assuming that  $\tau \sim 1/q$ . The dashed curve marked II is calculated assuming  $\tau(q) \sim 1/q^2$ .

not be reconciled with such a large value for  $\eta_D$ . Scrutinizing the accuracy of our measurements once again, the thermoelectric power measured by us may be a slight underestimate because of the manner in which we calculated the temperature gradient. The error in  $\Delta Q^e$  due to this is small, no more than 10% in the most unfavorable case, which can increase  $\eta_D$  by no more than 5%. Secondly, we believe that the electronic component of  $\Delta Q^e$  is given by our Eq. (3.1). An error of a few tens of microvolts/deg in  $\Delta Q^e$  is not of much significance since  $\Delta Q^e$  is several 1000  $\mu\text{V}/\text{deg}$ . On the other hand, assuming a value of 30 eV for  $\eta_D$ , if we estimate the phonon-drag thermoelectric power in the zero field (as done in Ref. 1) we get a value of  $\sim 800 \mu\text{V}/\text{deg}$  which should be observable, if correct. However, independent measurements of the thermoelectric power of  $n$ -InSb by different authors show a much smaller value, almost the whole of which can be accounted for by the electronic term.

Our second conclusion regarding electron-phonon scattering is that there is no interaction via the piezoelectric mode for  $T \geq 6^\circ\text{K}$ . The statement should be modified to say that the high-field phonon drag is not affected by piezoelectric scattering because, as the theory shows, the scattering in the piezoelectric mode is discriminated against. This is because in the quantum region the mean wavelength of phonons that interact with electrons continuously decreases with the magnetic field. The nature of interactions is such that the ratio of piezoelectric scattering to deformation-potential scattering decreases with the decrease in wavelengths of the phonons.

Our conclusions about the relaxation time of phonons are not in agreement with Herring's theory. Although the cubic dependence of the inverse of the relaxation time on temperature is in agreement with Herring's prediction, there are two points of disagreement. First, we find in Eq. (6.1) the value of  $m=1$  instead of the ideal value of two predicted by Herring. Also it has been predicted that the sum of the exponents  $r$  and  $m$  is always 5, while the sum of exponents in our case is 4. Deviations from the theoretical value 5 are expected only when the condition  $T \ll \theta_D$  (Debye temperature =  $205^\circ\text{K}$  for InSb) is violated. We have no explanation of these disagreements.

Finally, we wish to say a few words about the disagreement between the measured and the calculated values of  $\Delta Q^e$  for fields higher than 60 kG; the measured values are always less than the calculated values. There may be two reasons for this. First, we see that in a high magnetic field the wave vector  $q_p$  of phonon-drag phonons becomes comparable to  $q_t$  of thermal phonons. For example, at  $10^\circ\text{K}$ ,  $q_t \approx (kT/\hbar S)$

$= 3.7 \times 10^6 \text{ cm}^{-1}$ , which is only about three times  $q_p [\approx (eB/\hbar c)^{1/2}]$  at 100 kG. Our theory is in error in as far as the assumption  $q_t \gg q_p$  is violated in this case. The theory of phonon drag in extremely high magnetic fields when  $B \geq (\hbar c/e)(kT/\hbar S)^2$  has been discussed by Gurevich and Efros.<sup>37</sup> They predict that in this situation the thermoelectric power becomes independent of the magnetic field once again. Instead of the saturation predicted by them we observe that, at  $6.5^\circ\text{K}$ ,  $\Delta Q^e$  goes through its maximum value at 90 kG and starts decreasing as the field is increased further. Second, we observe that in the theory we have neglected the broadening of the electron-energy levels due to collisions. Collision broadening is one of the mechanisms invoked to remove divergence in the theory of magnetoresistance<sup>32</sup> in the quantum region. The inelasticity of electron-phonon collision is another. We have considered only the latter mechanism. Since the scattering rate increases with the field, it is possible that the collision broadening becomes dominant in high fields while the inelasticity of collisions dominates at low fields. The finite energy of the interacting phonons gives rise to the second exponential factor in Eq. (2.14) with the consequence that Eq. (2.13) remains finite for  $q_z=0$ . The electron energy states have a finite width  $\sim \hbar/\tau$  and a corresponding spread  $\Delta k_z$  in momentum along the magnetic field. A collision is not significant unless it changes  $k_z$  by an amount greater than  $\Delta k_z$  which means only phonons with  $q_z \geq \Delta k_z$  can take part in electron scattering. Collision broadening thus sets a finite lower limit to the integral over  $|q_z|$  and a corresponding lower limit  $x_{\min}$  in the integrals  $I_n$  of Eq. (5.4). If the value of  $x_{\min}$  is such that the factor  $\exp(-\nu/x_{\min}^2)$  of Eq. (5.4) which arises due to inelasticity, is already small, the effect of collision broadening will be negligible. In the opposite case a finite  $x_{\min}$  reduces the value of integral  $I_n$  and hence the calculated values of  $Q_p$ . The value of  $x_{\min}$  depends on the magnetic field because of its dependence on  $\tau$ . At present, the theory of collision broadening has not been worked out in the quantum region. It seems that for  $T \geq 20^\circ\text{K}$ , collision broadening may be responsible for low measured values in high fields, while for low temperatures the first explanation also plays a part.

#### ACKNOWLEDGMENTS

It is a pleasure to thank Dr. T. H. Geballe and Dr. C. Herring for their continued interest in the work and helpful discussions at various stages. I would also like to thank Professor C. F. Quate for his comments on the manuscript.